Atmos. Chem. Phys. Discuss., https://doi.org/10.5194/acp-2017-785
Manuscript under review for journal Atmos. Chem. Phys.
Discussion started: 25 August 2017

Atmospheric Chemistry and Physics Discussions

The single-particle mixing state and cloud scavenging of black carbon at a high-altitude mountain site in southern China

Guohua Zhang [1], Qinhao Lin [1, 2], Long Peng [1, 2], Xinhui Bi [1,*], Duohong Chen [3], Mei Li [4, 5], Lei Li [4, 5], Fred J. Brechtel [6], Jianxin Chen [7], Weijun Yan [7], Xinming Wang [1], Ping'an Peng [1], Guoying Sheng [1], Zhen Zhou [3]

[1]State Key Laboratory of Organic Geochemistry and Guangdong Key Laboratory of Environmental Resources Utilization and Protection, Guangzhou Institute of Geochemistry, Chinese Academy of Sciences, Guangzhou 510640, PR China

[2] Graduate University of Chinese Academy of Sciences, Beijing 100039, PR China

[3] State Environmental Protection Key Laboratory of Regional Air Quality Monitoring, Guangdong Environmental Monitoring Center, Guangzhou 510308, PR China

[4] Institute of Mass Spectrometer and Atmospheric Environment, Jinan University, Guangzhou 510632, China

[5] Guangdong Provincial Engineering Research Center for on-line source apportionment system of air pollution, Guangzhou 510632, China

[6] Brechtel Manufacturing Inc., Hayward, 94544, California, USA

[7] Shaoguan Environmental Monitoring Center, Shaoguan 512026, PR China

Correspondence should be addressed to Xinhui Bi (bixh@gig.ac.cn)

Atmos. Chem. Phys. Discuss., https://doi.org/10.5194/acp-2017-785
Manuscript under review for journal Atmos. Chem. Phys.
Discussion started: 25 August 2017

Atmospheric Chemistry and Physics Discussions

Highlights

- In situ investigation of both the mixing state and cloud scavenging of BC in China was first reported.
- Measured BC-containing particles were activated into cloud droplets to the same extent as all the measured particles due to being predominantly mixed with sulfate.
- BC-containing particles with higher fractions of organics were activated relatively less than those with higher fractions of sulfate.

Atmos. Chem. Phys. Discuss., https://doi.org/10.5194/acp-2017-785
Manuscript under review for journal Atmos. Chem. Phys.
Discussion started: 25 August 2017

Atmospheric Chemistry and Physics Discussions

Abstract

In the present study, a ground-based counterflow virtual impactor (GCVI) was used to sample cloud droplet residual (cloud RES) particles, while a parallel $PM_{2.5}$ inlet was used to sample cloud-free or cloud interstitial (cloud INT) particles. The mixing state of black carbon (BC)-containing particles in a size range of 0.1-1.6 μm and the mass concentrations of BC in the cloud-free, RES and INT particles were investigated using a single particle aerosol mass spectrometer (SPAMS) and two aethalometers, respectively, at a mountain site (1690 m a.s.l.) in southern China. The measured BC-containing particles were internally mixed extensively with sulfate, and were activated into cloud droplets to the same extent as all the measured particles. The results indicate the preferential activation of larger particles and/or that the production of secondary compositions shifts the BC-containing particles towards larger sizes. BC-containing particles with an abundance of both sulfate and organics were activated less than those with sulfate but limited organics, implying the importance of the mixing state on the incorporation of BC-containing particles into cloud droplets. The mass scavenging efficiency of BC with an average of 33% was similar for different cloud events independent of the air mass. This is the first time that both the mixing state and cloud scavenging of BC in China have been reported. Since limited information on BC-containing particles in the free troposphere is available, the results also provide an important reference for the representation of BC concentrations, properties, and climate impacts in modeling studies.

Keywords: black carbon, cloud droplet residues, mixing state, scavenging efficiency, interstitial particle

Atmos. Chem. Phys. Discuss., https://doi.org/10.5194/acp-2017-785
Manuscript under review for journal Atmos. Chem. Phys.
Discussion started: 25 August 2017

Atmospheric Chemistry and Physics Discussions

1 Introduction

Black carbon (BC), also known as soot or elemental carbon, is primarily emitted from incomplete combustion processes (Petzold et al., 2013; Bond et al., 2013). Fresh BC-containing particles are generally hydrophilic due to the presence of thin coatings of inorganic or organic materials (Zuberi et al., 2005), and during transport they become more hydrophilic when further coated through coagulation, condensation and photochemical oxidation (Zuberi et al., 2005; Zaveri et al., 2010; Matsui, 2016). Hydrophilic BC-containing particles can act as cloud condensation nuclei (CCN) and thus modify cloud microphysical properties (Straub et al., 2012; Schroder et al., 2015; Roth et al., 2016). The increase in CCN activity enhances the in-cloud scavenging of BC and thus reduces its lifetime (Zaveri et al., 2010). Aerosol-cloud interactions represent one of the largest uncertainties in our current understanding of human-induced climate forcing (McFiggans et al., 2006; Andreae and Rosenfeld, 2008). Therefore, a more comprehensive understanding of how aerosol particles form cloud droplets is required in order to reduce the uncertainty of the impacts of aerosols on the climate (Furutani et al., 2008).

The abilities of particles to act as CCN are largely controlled by their sizes and chemical compositions or mixing state (Dusek et al., 2006; Cubison et al., 2008; Kammermann et al., 2010; Ching et al., 2012; Baustian et al., 2012). Larger aerosol particles were found to be more easily activated into cloud droplets (Drewnick et al., 2007). Zhou et al. (2009) reported higher scavenging rates for sulfate, nitrate and BC than those for organics at Mount Tai in northern China. At the same site, 92% of the cloud residues were attributed to sulfate-related

salts (Li et al., 2011b). On the other hand, the chemical compositions of the original CCN would be altered after the evaporation of the cloud droplets through the effective formation of secondary aerosol compositions during cloud processing (Hayden et al., 2008; Herrmann et al., 2015; Roth et al., 2016). For BC-containing particles, the mixing state should be much more significant, since their activation as CCN is primarily attributed to the presence of secondary coatings (Lambe et al., 2015; Schroder et al., 2015). Additionally, the mixing state of BC-containing particles is complex and constantly changing in the atmosphere, and they are highly influenced by the particle size, sources, the formation of secondary species and transport processes (Cahill et al., 2012; Healy et al., 2012; Zhang et al., 2014).

Recent in situ studies of cloud droplets have provided the most direct information on the incorporation of BC into clouds. The mass scavenging efficiency was observed to be in a range of 33–74% for BC, which was higher with increasing particle sizes at the Puy de Dome (1465 m a.s.l.), France (Sellegri et al., 2003), while it ranged from 13% to 50% within different air masses at a coastal Chilean hill (450 m a.s.l.) (Heintzenberg et al., 2016). Cozic et al. (2007) reported a scavenging rate of BC similar to those of bulk aerosols due to its internal mixing state with soluble materials. Wang et al. (2012) showed a higher scavenging efficiency for BC than those for organics. Roth et al. (2016) found an enhanced contribution of BC-containing particles in cloud residues compared to that in interstitial particles. However, Zelenyuk et al. (2010) observed negligible BC in cloud droplet residues above Alaska, USA. Therefore, an in-depth study on the composition, size and mixing state of BC in cloud droplets and interstitial particles is requisite for a better understanding of the

interactions between BC and cloud droplets and the influences of anthropogenic emissions on cloud formation in the free troposphere.

Single-particle mass spectrometry (SPMS) studies on fog interstitial particles and droplet residual particles were performed previously at an urban site in southern China (Zhang et al., 2012; Bi et al., 2016). The predominance of BC-containing particles that serve as effective fog condensation nuclei highlights the important influence of anthropogenic emissions on the public environment and regional climate (Bi et al., 2016). However, there are no direct observations of the cloud scavenging of BC or the mixing states of cloud interstitial (cloud INT) and droplet residual (cloud RES) BC-containing particles in the high-altitude atmosphere or the free troposphere above China to date. Therefore, the size-resolved mixing state and the scavenging efficiency of BC-containing particles were investigated at a high-altitude site to further our knowledge of (1) the mixing state of BC-containing particles, (2) the influence of the mixing state on the incorporation of BC into cloud droplets, and (3) the influence of anthropogenic activities on cloud formation in the free troposphere above southern China.

2 Methods

2.1 Sampling setup

The observations of cloud events were conducted at the National Atmospheric Background Monitoring Station in Nanling of Guangdong Province, which is located on the top of Mount Tianjing (24°41′56″N, 112°53′56″E, 1690 m a.s.l.) in southern China, from 16

to 26 Jan 2016. The site is located in a natural preserve isolated from anthropogenic activities. A map of the location and terrain of the site can be found elsewhere (Lin et al., 2017).

Aerosols were introduced into the instruments through two parallel sampling lines. The first inlet is a ground-based counterflow virtual impactor (GCVI) (Model 1205, Brechtel Mfg., Inc., USA) (Bi et al., 2016). The GCVI employs a compact wind tunnel upstream of the CVI inlet (Model 1204) (Shingler et al., 2012) to accelerate fog and cloud droplets into the CVI inlet tip. Similar methodologies have been extensively applied to collect fog/cloud RES particles (e.g., Sorooshian et al., 2013; Roth et al., 2016; van Pinxteren et al., 2016). Upstream of the CVI sampling tip, only the droplets that exceed 8 μm can pass through the counterflow. The sampled cloud droplets enter the evaporation chamber (with an airflow temperature of 40 °C), where the droplets are dried, thereby leaving behind cloud RES particles that are capable of acting as CCN. A testing before measurements demonstrates that the influence of background aerosols on the collection of cloud droplets could be negligible (Zhang et al., 2017). The ambient inlet is a $PM_{2.5}$ sampling line that delivers ambient particles during cloud-free periods or cloud INT particles during cloud events. Cloud INT particles were regarded as $PM_{2.5}$ during the cloud events. More detailed description on the sampling can be found in the companion papers (Lin et al., 2017; Zhang et al., 2017).

Cloud events were characterized by a sudden drop in visibility and a sharp increase in the relative humidity (RH) measured by the GCVI. An upper-limit visibility threshold of 5 km and a lower-limit RH threshold of 95% were established to identify the cloud events and

trigger the sampling of the cloud RES particles. A rainfall detector within the GCVI system was used to exclude rainy periods. The enhancement factor (EF) for the particles collected by the GCVI is 5.25 (Shingler et al., 2012). Therefore, the reported mass concentrations for the cloud RES particles in the following text were first divided by 5.25.

An illustrative scheme of the instrumentation setup is provided in Fig. S1 in the Supporting Information (SI). Downstream of the GCVI, an aethalometer (Model AE-33, Magee Scientific, USA), a single particle aerosol mass spectrometer (SPAMS, Hexin Analytical Instrument Co., Ltd.) and a scan mobility particle sizer (SMPS, MSP Corporation, USA) were used to measure the concentration of BC, the size-resolved mixing state of the collected particles, and the number size distribution of submicron particles, respectively. Downstream of the ambient inlet, an SMPS (Grimm 5.041, Germany), an aethalometer (Model AE-31, Magee Scientific, USA), and a tapered element oscillating microbalance (Model 1405, TEOM) were used to determine the number size distribution of submicron particles and the mass concentrations of BC and $PM_{2.5}$, respectively. During the cloud-free periods, the instruments downstream of the GCVI were manually shifted and connected to the ambient $PM_{2.5}$ inlet. During the present study, three cloud events (Cloud I, II, III, each with a RH constantly above 95% for more than 12 hours) were encountered and identified by the GCVI (Lin et al., 2017), as shown in Fig. 1. During Cloud I and II, the cloud RES particles provided by the GCVI were measured by the instruments downstream of the GCVI. During Cloud III, the cloud RES and cloud INT particles were intermittently measured by these instruments at approximately one-hour intervals.

157

158 **2.2 Determinations of the mass concentrations of BC**

159 The AE–31 and AE–33 measured the BC concentration at seven different wavelengths
160 (370, 450, 520, 590, 660, 880 and 950 nm), which are typically represented as equivalent BC
161 (EBC) (Petzold et al., 2013). The measurements are based on the light beam attenuation
162 (ATN) on a filter, which is proportional to the loading of the BC deposit. In this study, the
163 ATN was converted to an EBC concentration at the wavelength of 880 nm. The EBC
164 concentration reported in the present study was measured using the AE–33, which was
165 described in great detail (Drinovec et al., 2015). The limitations and uncertainties of the
166 AE-31 in measuring BC and the necessary corrections were well documented (Weingartner
167 et al., 2003; Arnott et al., 2005; Backman et al., 2016). A brief description of this issue is
168 provided in the Supplement.

169

170 **2.3 Identification of BC-containing particles by the SPAMS**

171 Both the vacuum aerodynamic diameter (d_{va}) and the chemical compositions of the
172 individual particles were analyzed by the SPAMS, as briefly described in the supplement. A
173 detailed description of the performance of the SPAMS can be found elsewhere (Li et al.,
174 2011a). The mass spectra for approximately 75000 particles with d_{va} values in the range of
175 0.1-1.6 μm were obtained by the SPAMS over the study. The diameter is represented herein
176 as d_{va} rather than the equivalent volume diameter (d_{ve}), the conversion for which can be
177 found in the supplement (DeCarlo et al., 2004; Hu et al., 2012). An adaptive resonance

178 theory-based neural network algorithm (ART-2a) was applied to cluster the individual
179 particles based on the presence and intensities of ion peaks (Song et al., 1999) with a
180 vigilance factor of 0.7, a learning rate of 0.05, and 20 iterations. Three BC particle types
181 were obtained: the mass spectra of particles with more carbon cluster ions ($C_n^{+/-}$, $n > 6$) and
182 sulfate (BC-sul1), those with fewer carbon cluster ions ($C_n^{+/-}$, $n \leq 6$) and more intense
183 sulfate (BC-sul2), and those with an abundance of both sulfate and organics (BC-OC-sul).
184 The relative amount of OC to BC for the BC-OC-sul particles is significantly larger than
185 the relative amount of OC in the BC-sul1 and BC-sul2 particles, as indicated in Fig. S2.
186 Over all of the detected BC-containing particles, the BC-sul2 type is the most abundant
187 (63%) particle type, followed by the BC-sul1 (21%) and BC-OC-sul (16%) types. More
188 detailed information regarding the other particle types can be found elsewhere (Lin et al.,
189 2017).
190
191 **3 Results and Discussion**
192 During the sampling periods, the temperature and RH generally varied between –9.9 -
193 11.4 °C and 6.7 - 100%, respectively. The sampling durations for the cloud-free, cloud RES
194 and cloud INT (only detected in Cloud III) particles were approximately 109, 123, and 26
195 hours, respectively. The detected numbers of the cloud-free, cloud RES, and cloud INT
196 particles by the SPAMS were 48835, 23616, and 1063, respectively. The average number
197 fractions of BC-containing particles in the cloud-free, cloud RES, and cloud INT particles in
198 the size range of d_{va} = 0.1-1.6 μm were 44%, 49%, and 53%, respectively. The number

199 fractions of BC-containing particles that were incorporated within the cloud droplets ranged
200 between those observed at an urban site (70%) in southern China (Bi et al., 2016) and those
201 observed at a mountain site (~30%) in Germany (Roth et al., 2016). While some mineral dust
202 might trigger heterogeneous ice nucleation at temperatures below –7 °C (Atkinson et al.,
203 2013), this would not influence the discussion on the number fraction and chemistry of the
204 cloud RES BC-containing particles. The sampling duration of the cloud RES particles with
205 an average temperature of ~ –7 °C only lasted 2 hours, during which the detected cloud RES
206 BC-containing particles only accounted for ~0.1% of all the detected ones.
207 Air masses from the southwestern continental and marine areas dominated throughout
208 the sampling period, carrying relatively warmer and wetter air masses that benefited the
209 formation of clouds based on the back-trajectory analysis (Lin et al., 2017). Cloud II was
210 strongly influenced by a northeastern air mass in contrast to the southwestern air mass that
211 dominated during Cloud I and III. As shown in Fig. 2, the air mass during Cloud II
212 represents relatively polluted conditions. The mass concentration of EBC during Cloud II
213 was approximate 200 ng m^{-3}, which is four times that (~50 ng m^{-3}) observed during the
214 other two events. Similarly, the number fraction of the BC-containing particles in the cloud
215 RES particles during Cloud II (~60%) was higher than those during the other two cloud
216 events (< 30%). These results provide direct evidence for the influence of anthropogenic
217 emissions and atmospheric transport on the formation of clouds at the remote high-altitude
218 site in southern China.
219

Atmos. Chem. Phys. Discuss., https://doi.org/10.5194/acp-2017-785
Manuscript under review for journal Atmos. Chem. Phys.
Discussion started: 25 August 2017

Atmospheric Chemistry and Physics Discussions

3.1 Mixing state of BC for cloud-free, residual, and interstitial particles

The dominant ion peaks for the cloud-free, cloud RES, and cloud INT BC-containing particles were those of carbon cluster ions ($C_n^{+/-}$, n = 1, 2, 3, …), OC fragments (m/z 27$[C_2H_3]^+$, -26$[CN]^-$, 37$[C_3H]^+$, and 43$[C_2H_3O]^+$), and secondary inorganic species, such as sulfate (-97$[HSO_4]^-$), nitrate (-62$[NO_3]^-$ and -46$[NO_2]^-$), and ammonium (18$[NH_4]^+$) (Zhang et al., 2014). The cloud-free BC-containing particles were internally mixed to a great extent with detectable sulfate (97% in number), nitrate (50%), oxidized organics (72%), and/or ammonium (79%), as presented in Fig. S3. The oxidized organics were generally represented as the peak at m/z 43$[C_2H_3O]^+$ in SPMS studies (Qin et al., 2012). A similar mixing state of the BC-containing particles has been observed at both urban and mountain sites (Moffet and Prather, 2009; Li et al., 2011c; Cahill et al., 2012). The overwhelming association of BC with sulfate strongly indicates a substantial influence of anthropogenic emissions of sulfate precursors (e.g., SO_2) on the aging of BC (Huang and Yu, 2008; Khalizov et al., 2009; Guo et al., 2012; Peng et al., 2016), which directly enhances the incorporation of BC into clouds as discussed in section 3.2. Compared to the BC-containing particles at urban and suburban sites that are situated close to emission sources, the relative amounts of sulfate and ammonium substantially increased for those at the mountain site, as shown in Fig. S4. The relative peak area (RPA) of each m/z relative to the sum of the peak areas in a mass spectrum was applied herein to represent the relative amount of a species in a particle (e.g., Xing et al., 2011; Jeong et al., 2011; Healy et al., 2013). The enhancement of sulfate in the atmosphere above southern China is reasonable since sulfate accounts for the

largest portion of the compositions in this region and should be mainly associated with ammonium (Zhang et al., 2013). As expected, the temporal variations of the RPAs were significantly correlated ($p < 0.01$) between ammonium and sulfate (Fig. S5). These species were generally regarded as secondary components, and thus, such high fractions of the internal mixing state and the enhancement of ammonium and sulfate at the high-altitude site indicates a highly aged state of the BC-containing particles.

As shown in Fig. 3, the secondary components were enhanced in the cloud RES BC-containing particles relative to the cloud INT BC-containing particles. The enhancement was more obvious for sulfate rather than for ammonium, oxidized organics or nitrate. The enhancement of sulfate in cloud RES particles has been broadly observed (Zelenyuk et al., 2010; Kamphus et al., 2010; Hiranuma et al., 2011). A comparison of the size distributions of the cloud RES and cloud INT BC-containing particles (Fig. 4) further suggests that the in-cloud addition of secondary components shifted the BC-containing particles towards larger sizes, which is discussed in the following section. Overall, our observations suggest that the BC-containing particles were heavily coated at the high-altitude site before they were incorporated into the cloud droplets and that the in-cloud production of coating materials (e.g., ammonium sulfate) was present. An abundance of BC-coated materials was also observed at Mt. Soledad (Schroder et al., 2015). Unfortunately, their chemical compositions cannot be ruled out by a single particle soot photometer. Therefore, our analysis reflects the importance of the chemical mixing state on the cloud processing of BC.

262

263 **3.2 Fractions of BC incorporated into cloud droplets**

264 **3.2.1 Size-resolved activation of BC-containing particles**

265 The normalized number size distributions of the cloud-free, cloud RES, and cloud INT
266 BC-containing particles are shown in Fig. 4. While these distributions do not represent the
267 actual particle number size distributions, they could reflect the importance of the particle
268 size on the incorporation of BC-containing particles into cloud droplets (Dusek et al., 2006).
269 The cloud RES BC-containing particles had the largest size mode, followed by the
270 cloud-free BC-containing particles with the cloud INT BC-containing particles in the
271 smallest size mode. These size distribution patterns are consistent with those of previous
272 studies (Zelenyuk et al., 2010; Drewnick et al., 2007; Roth et al., 2016), which are indicative
273 of the preferential activation of larger particles and/or the addition of secondary species
274 during in-cloud processing (Schroder et al., 2015). As expected, the BC-containing particles
275 were internally mixed with increasingly higher intensities of sulfate, ammonium and
276 oxidized organics with increasing size (Fig. S6). These results are consistent with the
277 observations by Healy et al. (2012) and Zhang et al. (2014) insomuch that larger
278 BC-containing particles were more thickly coated. The BC-containing particles detected by
279 the SPAMS could track the variations of the BC mass concentration in the present study
280 based on a correlation analysis of the time series of the unscaled number of BC-containing
281 particles and the concentration of EBC (Fig. S7). A detailed discussion on the comparison of

these two measurements can be found in the supplement (Yu et al., 2010; Huang et al., 2011; Huang et al., 2012).

The size-resolved activated fractions (Nf_{act}) of the BC-containing particles and all the detected particles were further investigated as a function of their size (Fig. 5). The Nf_{act} generally increased with an increase in the size, and those of the BC-containing particles were activated to a similar (or slightly lower) extent as those of all the detected particles. This indicates that the coating materials on the BC-containing particles enhanced their ability to act as CCN (Khalizov et al., 2009; Henning et al., 2012; Roth et al., 2016), which is also consistent with the enhanced internal mixing with secondary soluble species with an increase in the size (Fig. S6) discussed above. The increase of Nf_{act} with the particle size also suggests that nucleation scavenging is the dominant mechanism for the incorporation of BC-containing particles into cloud droplets (Schroder et al., 2015). The number fractions of the BC-containing particles incorporated into cloud droplets varied between 0.05–0.45 (Fig. 5). These fractions represent a rough estimate because the BC-containing particles in the cloud RES and cloud INT particles were measured intermittently rather than simultaneously. Henning et al. (2002) showed that particles with d_{ve} = 700 nm were only half activated in less dense clouds (with a liquid water content or LWC < 0.1 g m^{-3}), while their diameter decreased to ~100 nm when the LWC > 0.2 g m^{-3} at a high-alpine site. Similarly, Hammer et al. (2014) showed that only particles with a d_{ve} larger than 300 - 500 nm could be activated under low-LWC conditions (LWC < 0.1 g m^{-3}), which is a common condition for the formation of fog at the ground level. With an LWC of approximately 0.1

303 g m^{-3}, Schroder et al. (2015) reported even lower activated fractions (0.01–0.1) of
304 BC-containing particles at Mt. Soledad closer to the source region in California, USA.
305 From this perspective, the relatively higher activation fractions of the BC-containing
306 particles in the present study compared to those at Mt. Soledad (Schroder et al., 2015) could
307 be mainly attributed to the long-range transport that resulted in the highly aged BC and
308 possibly the higher LWC.

309 The role of the mixing state on the activation of the BC-containing particles was
310 further investigated through a comparison of the individual particle types of the cloud-free,
311 cloud RES, and cloud INT BC-containing particles. As shown in Fig. 6, the number
312 fraction of BC-OC-sul was much lower in the cloud RES (~8%) than those (~25%) in the
313 cloud-free and cloud INT BC-containing particles. Despite the different distributions of the
314 BC particle types, the BC-sul1 and BC-sul2 types were dominant, while the BC-OC-sul type
315 contributed only a limited fraction to the cloud RES BC-containing particles during each of
316 the cloud events. Consistently, the Nf_{act} of the BC-OC-sul particles was generally lower
317 than 0.1 over the detected size range, which is much lower than those for the BC-sul1 and
318 BC-sul2 types (Fig. S8). Furthermore, the organic-dominated particle types (organics
319 internally mixed with sulfate and negligible BC (Lin et al., 2017)) in all the detected
320 particles was activated to a lesser extent, as presented in Fig. S9. Distinct differences in the
321 mixing state accompanied the observations of cloud RES BC-containing particles.
322 BC-containing residuals with more sulfate and fewer organics were observed more
323 frequently than those with more organics and less sulfate.

324

325 **3.2.2 Mass scavenging efficiency of EBC**

326 The concentration of EBC (5^{th} - 95^{th}) obtained using the AE33 for cloud-free air varied
327 over a wide range of 57 - 812 ng m^{-3} with a mean value of 418 ± 248 ng m^{-3}, which accounted
328 for ~2% of the $PM_{2.5}$ on average. The average concentrations of cloud RES and INT EBC
329 were 84 ± 75, and 198 ± 125 ng m^{-3}, respectively. A relatively lower contribution of EBC to
330 the aerosol population supports a substantial addition of secondary aerosols during
331 transport to the high-altitude site, given that EBC represents far more than ~2% of the fine
332 particles near the source regions of southern China (Lan et al., 2013; Wu et al., 2013;
333 Zhang et al., 2013). The observed relatively lower fraction of EBC is consistent with the
334 highly aged state of BC-containing particles at the high-altitude site rather than at urban
335 and suburban sites, as discussed in section 3.1. The mean concentration is much lower than
336 those observed for urban (6000 ng m^{-3}) and rural (2600 ng m^{-3}) areas (Huang et al., 2012),
337 it is similar to those observed at an oceanic site (540 ng m^{-3}) in southern China (Wu et al.,
338 2013) and at the high-altitude Mt. Rax site (430-720 ng m^{-3}) (Hitzenberger et al., 2001),
339 and it is several times higher than those at a marine boundary layer site (70 ng m^{-3}) in
340 California, USA (Schroder et al., 2015), the mid-altitude regions (~60 ng m^{-3}) of Nova
341 Scotia, Canada (Chýlek et al., 1996), and the high alpine Jungfraujoch station (50-60 ng
342 m^{-3}) in Switzerland (Cozic et al., 2007). Additional detailed information on the sampling
343 sites and BC concentrations can be found in Table S1. These comparisons suggest that

344 anthropogenic activities have a relatively large impact on the concentration of EBC at the
345 high-altitude site.

346 It can be seen from Fig. 1 that cloud scavenging could have a strong effect on the
347 decreased particle concentrations (i.e., of EBC and $PM_{2.5}$). A sharp reduction in the particle
348 concentrations were observed at the beginning of the cloud events. The mass-scavenging
349 efficiency of BC ($Mf_{scav,EBC}$), defined as the fraction of EBC incorporated into cloud
350 droplets relative to the total amount of EBC (Cozic et al., 2007), was evaluated as

351 $$Mf_{scav,EBC} = EBC_{RES}/(EBC_{RES} + EBC_{INT}) \times 100\% \quad (R1)$$

352 Since the EBC_{RES} and EBC_{INT} were not simultaneously obtained using the AE-33, the
353 EBC_{INT} measured concurrently by the AE-31 was applied in the calculation. The EBC
354 measured using the AE-31 is significantly correlated ($R^2 = 0.9$, $p < 0.001$) with and only
355 slightly lower than that measured by the AE-33, as shown in Fig. S10. This validates the
356 calculation in R1. The overall uncertainty in the $Mf_{scav,EBC}$ is within 10%, as assessed in the
357 supplement. The measurements of EBC and the sampling of the cloud RES particles were
358 regarded as the main influential factors.

359 The $Mf_{scav,EBC}$ ranged between 15 - 54% (5^{th} - 95^{th}) with an average of approximately
360 33%. The $Mf_{scav,EBC}$ in this study is within the range of those values (33-54%) reported for
361 mid-altitude (approximately 1500 m) mountain sites, generally lower than those reported
362 (45-74%) for high-altitude (approximately 3000 m) mountain sites, and higher than those
363 reported (6-15%) for ground sites (Cozic et al., 2007 and references therein). The
364 differences among the various observations are generally attributed to the water content

and the sizes and mixing state of the BC-containing particles (Cozic et al., 2007). The $Mf_{scav,EBC}$ was not so different for the cloud events (Fig. S11) impacted by different air masses, which is consistent with the highly aged state of the BC observed in this study. These results indicate that the incorporation of BC into clouds was dominantly controlled by its mixing state rather than other factors (e.g., the air mass or the concentration of EBC) under low-LWC conditions (e.g., < 0.1 g m^{-3}).

4 Conclusions

The influences of the size and mixing state on the incorporation of BC in clouds were investigated at a remote high-altitude mountain site in southern China. On average, the mass concentration of EBC was 418 ± 248, 84 ± 75, and 198 ± 125 ng m^{-3} for cloud-free, cloud RES, and cloud INT particles, respectively. The BC was highly aged through the predominant accumulation of sulfate during transport. BC-containing particles were found to be scavenged in the cloud phase to a similar extent as bulk aerosols. The size-resolved activation fraction of BC-containing particles was estimated to be in the range of 0.05–0.45; it increased with an increase in the size and was mainly controlled by the mixing state with secondary soluble species. Our results are restricted to particles in the size range of 0.1-1.6 μm, and thus, particles with sizes smaller than 0.1 μm that might serve as CCN are beyond the scope of this study. The mass-scavenging efficiency of BC varied between 15–54% and was independent of the air mass. This paper provides the first direct evidence on the substantial contribution of BC-containing particles to cloud droplet residues in the free

troposphere of southern China. The data are also useful for constraining models used for predicting BC concentrations in the free troposphere.

Acknowledgement

This work was supported by the National Key Research and Development Program of China (2017YFC0210104), the National Natural Science Foundation of China (No. 91544101 and 41775124), the Foundation for Leading Talents of the Guangdong Province Government, and the State Key Laboratory of Organic Geochemistry (SKLOGA201603A and SKLOGC201604).

References

Allen, J. O., Fergenson, D. P., Gard, E. E., Hughes, L. S., Morrical, B. D., Kleeman, M. J., Gross, D. S., Galli, M. E., Prather, K. A., and Cass, G. R.: Particle detection efficiencies of aerosol time of flight mass spectrometers under ambient sampling conditions, Environ. Sci. Technol., 34, 211-217, 2000.

Andreae, M. O., and Rosenfeld, D.: Aerosol–cloud–precipitation interactions. Part 1. The nature and sources of cloud-active aerosols, Earth-Sci. Rev., 89, 13-41, doi:http://dx.doi.org/10.1016/j.earscirev.2008.03.001, 2008.

Arnott, W. P., Hamasha, K., Moosmuller, H., Sheridan, P. J., and Ogren, J. A.: Towards aerosol light-absorption measurements with a 7-wavelength Aethalometer: Evaluation with a photoacoustic instrument and 3-wavelength nephelometer, Aerosol Sci. Tech., 39, 17-29, doi:10.1080/027868290901972, 2005.

Atkinson, J. D., Murray, B. J., Woodhouse, M. T., Whale, T. F., Baustian, K. J., Carslaw, K. S., Dobbie, S., O'Sullivan, D., and Malkin, T. L.: The importance of feldspar for ice nucleation by mineral dust in mixed-phase clouds, Nature, 498, 355-358, doi:10.1038/nature12278, 2013.

Backman, J., Schmeisser, L., Virkkula, A., Ogren, J. A., Asmi, E., Starkweather, S., Sharma, S., Eleftheriadis, K., Uttal, T., Jefferson, A., Bergin, M., and Makshtas, A.: On Aethalometer measurement uncertainties and multiple scattering enhancement in the Arctic, Atmos. Meas. Tech. Discuss., 2016, 1-31, doi:10.5194/amt-2016-294, 2016.

Baustian, K. J., Cziczo, D. J., Wise, M. E., Pratt, K. A., Kulkarni, G., Hallar, A. G., and Tolbert, M. A.: Importance of aerosol composition, mixing state, and morphology for heterogeneous ice nucleation: A combined field and laboratory approach, J. Geophys. Res., 117, 2240-2260, doi:10.1029/2011jd016784, 2012.

Bi, X. H., Lin, Q. H., Peng, L., Zhang, G. H., Wang, X. M., Brechtel, F. J., Chen, D. H., Li, M., Peng, P. A., Sheng, G. Y., and Zhou, Z.: In situ detection of the chemistry of individual fog droplet residues in the Pearl River Delta region, China, J. Geophys. Res.-Atmos., 121, 9105-9116, doi:10.1002/2016JD024886, 2016.

Bond, T. C., Doherty, S. J., Fahey, D. W., Forster, P. M., Berntsen, T., DeAngelo, B. J., Flanner, M. G., Ghan, S., Karcher, B., Koch, D., Kinne, S., Kondo, Y., Quinn, P. K., Sarofim, M. C., Schultz, M. G., Schulz, M., Venkataraman, C., Zhang, H., Zhang, S., Bellouin, N., Guttikunda, S. K., Hopke, P. K., Jacobson, M. Z., Kaiser, J. W., Klimont, Z., Lohmann, U., Schwarz, J. P., Shindell, D., Storelvmo, T., Warren, S. G., and Zender, C. S.: Bounding the role of black carbon in the climate system: A scientific assessment, J. Geophys. Res.-Atmos., 118, 5380-5552, doi:10.1002/Jgrd.50171, 2013.

Cahill, J. F., Suski, K., Seinfeld, J. H., Zaveri, R. A., and Prather, K. A.: The mixing state of carbonaceous aerosol particles in northern and southern California measured during CARES and CalNex 2010, Atmos. Chem. Phys., 12, 10989-11002, doi:10.5194/acp-12-10989-2012, 2012.

Chýlek, P., Banic, C. M., Johnson, B., Damiano, P. A., Isaac, G. A., Leaitch, W. R., Liu, P. S. K., Boudala, F. S., Winter, B., and Ngo, D.: Black carbon: Atmospheric concentrations and cloud water content measurements over southern Nova Scotia, J. Geophys. Res.-Atmos., 101, 29105-29110, doi:10.1029/95JD03433, 1996.

Ching, J., Riemer, N., and West, M.: Impacts of black carbon mixing state on black carbon nucleation scavenging: Insights from a particle-resolved model, J. Geophys. Res.-Atmos., 117, 1-21, 2012.

Cozic, J., Verheggen, B., Mertes, S., Connolly, P., Bower, K., Petzold, A., Baltensperger, U., and Weingartner, E.: Scavenging of black carbon in mixed phase clouds at the high alpine site Jungfraujoch, Atmos. Chem. Phys., 7, 1797-1807, 2007.

Cubison, M. J., Ervens, B., Feingold, G., Docherty, K. S., Ulbrich, I. M., Shields, L., Prather, K., Hering, S., and Jimenez, J. L.: The influence of chemical composition and mixing state of Los Angeles urban aerosol on CCN number and cloud properties, Atmos. Chem. Phys., 8, 5649-5667, 2008.

DeCarlo, P. F., Slowik, J. G., Worsnop, D. R., Davidovits, P., and Jimenez, J. L.: Particle morphology and density characterization by combined mobility and aerodynamic diameter

measurements. Part 1: Theory, Aerosol Sci. Tech., 38, 1185-1205, doi:10.1080/027868290903907, 2004.

Drewnick, F., Schneider, J., Hings, S. S., Hock, N., Noone, K., Targino, A., Weimer, S., and Borrmann, S.: Measurement of ambient, interstitial, and residual aerosol particles on a mountaintop site in central Sweden using an aerosol mass spectrometer and a CVI, J. Atmos. Chem., 56, 1-20, doi:10.1007/s10874-006-9036-8, 2007.

Drinovec, L., Močnik, G., Zotter, P., Prévôt, A. S. H., Ruckstuhl, C., Coz, E., Rupakheti, M., Sciare, J., Müller, T., Wiedensohler, A., and Hansen, A. D. A.: The "dual-spot" Aethalometer: an improved measurement of aerosol black carbon with real-time loading compensation, Atmos. Meas. Tech., 8, 1965-1979, doi:10.5194/amt-8-1965-2015, 2015.

Dusek, U., Frank, G. P., Hildebrandt, L., Curtius, J., Schneider, J., Walter, S., Chand, D., Drewnick, F., Hings, S., Jung, D., Borrmann, S., and Andreae, M. O.: Size matters more than chemistry for cloud-nucleating ability of aerosol particles, Science, 312, 1375-1378, doi:10.1126/science.1125261, 2006.

Furutani, H., Dall'osto, M., Roberts, G. C., and Prather, K. A.: Assessment of the relative importance of atmospheric aging on CCN activity derived from field observations, Atmos. Environ., 42, 3130-3142, doi:10.1016/j.atmosenv.2007.09.024, 2008.

Guo, J., Wang, Y., Shen, X. H., Wang, Z., Lee, T., Wang, X. F., Li, P. H., Sun, M. H., Collett, J. L., Wang, W. X., and Wang, T.: Characterization of cloud water chemistry at Mount Tai, China: Seasonal variation, anthropogenic impact, and cloud processing, Atmos. Environ., 60, 467-476, doi:10.1016/j.atmosenv.2012.07.016, 2012.

Hammer, E., Gysel, M., Roberts, G. C., Elias, T., Hofer, J., Hoyle, C. R., Bukowiecki, N., Dupont, J. C., Burnet, F., Baltensperger, U., and Weingartner, E.: Size-dependent particle activation properties in fog during the ParisFog 2012/13 field campaign, Atmos. Chem. Phys., 14, 10517-10533, doi:10.5194/acp-14-10517-2014, 2014.

Hayden, K. L., Macdonald, A. M., Gong, W., Toom-Sauntry, D., Anlauf, K. G., Leithead, A., Li, S. M., Leaitch, W. R., and Noone, K.: Cloud processing of nitrate, J. Geophys. Res.-Atmos., 113, 1-18, doi:10.1029/2007jd009732, 2008.

Healy, R. M., Sciare, J., Poulain, L., Kamili, K., Merkel, M., Muller, T., Wiedensohler, A., Eckhardt, S., Stohl, A., Sarda-Esteve, R., McGillicuddy, E., O'Connor, I. P., Sodeau, J. R., and Wenger, J. C.: Sources and mixing state of size-resolved elemental carbon particles in a European megacity: Paris, Atmos. Chem. Phys., 12, 1681-1700, doi:10.5194/acp-12-1681-2012, 2012.

Healy, R. M., Sciare, J., Poulain, L., Crippa, M., Wiedensohler, A., Prevot, A. S. H., Baltensperger, U., Sarda-Esteve, R., McGuire, M. L., Jeong, C. H., McGillicuddy, E., O'Connor, I. P., Sodeau, J. R., Evans, G. J., and Wenger, J. C.: Quantitative determination of carbonaceous particle mixing state in Paris using single-particle mass spectrometer and aerosol mass spectrometer measurements, Atmos. Chem. Phys., 13, 9479-9496, doi:10.5194/acp-13-9479-2013, 2013.

Heintzenberg, J., Cereceda-Balic, F., Vidal, V., and Leck, C.: Scavenging of black carbon in Chilean coastal fogs, Sci. Total. Environ., 541, 341-347, 2016.

Henning, S., Weingartner, E., Schmidt, S., Wendisch, M., Gaggeler, H. W., and Baltensperger, U.: Size-dependent aerosol activation at the high-alpine site Jungfraujoch (3580 m asl), Tellus B, 54, 82-95, 2002.

Henning, S., Ziese, M., Kiselev, A., Saathoff, H., Mohler, O., Mentel, T. F., Buchholz, A., Spindler, C., Michaud, V., Monier, M., Sellegri, K., and Stratmann, F.: Hygroscopic growth and droplet activation of soot particles: uncoated, succinic or sulfuric acid coated, Atmos. Chem. Phys., 12, 4525-4537, doi:10.5194/acp-12-4525-2012, 2012.

Herrmann, H., Schaefer, T., Tilgner, A., Styler, S. A., Weller, C., Teich, M., and Otto, T.: Tropospheric Aqueous-Phase Chemistry: Kinetics, Mechanisms, and Its Coupling to a Changing Gas Phase, Chem. Rev., 115, 4259-4334, doi:10.1021/cr500447k, 2015.

Hiranuma, N., Kohn, M., Pekour, M. S., Nelson, D. A., Shilling, J. E., and Cziczo, D. J.: Droplet activation, separation, and compositional analysis: laboratory studies and atmospheric measurements, Atmos. Meas. Tech., 4, 2333-2343, doi:10.5194/amt-4-2333-2011, 2011.

Hitzenberger, R., Berner, A., Glebl, H., Drobesch, K., Kasper-Giebl, A., Loeflund, M., Urban, H., and Puxbaum, H.: Black carbon (BC) in alpine aerosols and cloud water - concentrations and scavenging efficiencies, Atmos. Environ., 35, 5135-5141, 2001.

Hu, M., Peng, J. F., Sun, K., Yue, D. L., Guo, S., Wiedensohler, A., and Wu, Z. J.: Estimation of Size-Resolved Ambient Particle Density Based on the Measurement of Aerosol Number, Mass, and Chemical Size Distributions in the Winter in Beijing, Environ. Sci. Technol., 46, 9941-9947, doi:10.1021/Es204073t, 2012.

Huang, X. F., and Yu, J. Z.: Size distributions of elemental carbon in the atmosphere of a coastal urban area in South China: characteristics, evolution processes, and implications for the mixing state, Atmos. Chem. Phys., 8, 5843-5853, 2008.

Huang, X. F., Gao, R. S., Schwarz, J. P., He, L. Y., Fahey, D. W., Watts, L. A., McComiskey, A., Cooper, O. R., Sun, T. L., Zeng, L. W., Hu, M., and Zhang, Y. H.: Black carbon measurements in the Pearl River Delta region of China, J. Geophys. Res., 116, 445-451, doi:10.1029/2010jd014933, 2011.

Huang, X. F., Sun, T. L., Zeng, L. W., Yu, G. H., and Luan, S. J.: Black carbon aerosol characterization in a coastal city in South China using a single particle soot photometer, Atmos. Environ., 51, 21-28, doi:10.1016/j.atmosenv.2012.01.056, 2012.

Jeong, C. H., McGuire, M. L., Godri, K. J., Slowik, J. G., Rehbein, P. J. G., and Evans, G. J.: Quantification of aerosol chemical composition using continuous single particle measurements, Atmos. Chem. Phys., 11, 7027-7044, doi:10.5194/acp-11-7027-2011, 2011.

Kammermann, L., Gysel, M., Weingartner, E., Herich, H., Cziczo, D. J., Holst, T., Svenningsson, B., Arneth, A., and Baltensperger, U.: Subarctic atmospheric aerosol composition: 3. Measured and modeled properties of cloud condensation nuclei, J. Geophys. Res.-Atmos., 115, 288-303, doi:10.1029/2009jd012447, 2010.

Kamphus, M., Ettner-Mahl, M., Klimach, T., Drewnick, F., Keller, L., Cziczo, D. J., Mertes, S., Borrmann, S., and Curtius, J.: Chemical composition of ambient aerosol, ice residues and cloud droplet residues in mixed-phase clouds: single particle analysis during the

Cloud and Aerosol Characterization Experiment (CLACE 6), Atmos. Chem. Phys., 10, 8077-8095, doi:10.5194/acp-10-8077-2010, 2010.

Khalizov, A. F., Zhang, R. Y., Zhang, D., Xue, H. X., Pagels, J., and McMurry, P. H.: Formation of highly hygroscopic soot aerosols upon internal mixing with sulfuric acid vapor, J. Geophys. Res.-Atmos., 114, 730-734, doi:10.1029/2008jd010595, 2009.

Lambe, A. T., Ahern, A. T., Wright, J. P., Croasdale, D. R., Davidovits, P., and Onasch, T. B.: Oxidative aging and cloud condensation nuclei activation of laboratory combustion soot, J. Aerosol Sci., 79, 31-39, 2015.

Lan, Z. J., Huang, X. F., Yu, K. Y., Sun, T. L., Zeng, L. W., and Hu, M.: Light absorption of black carbon aerosol and its enhancement by mixing state in an urban atmosphere in South China, Atmos. Environ., 69, 118-123, doi:10.1016/j.atmosenv.2012.12.009, 2013.

Li, L., Huang, Z. X., Dong, J. G., Li, M., Gao, W., Nian, H. Q., Fu, Z., Zhang, G. H., Bi, X. H., Cheng, P., and Zhou, Z.: Real time bipolar time-of-flight mass spectrometer for analyzing single aerosol particles, Intl. J. Mass. Spectrom., 303, 118-124, doi:10.1016/j.ijms.2011.01.017, 2011a.

Li, W. J., Li, P. R., Sun, G. D., Zhou, S. Z., Yuan, Q., and Wang, W. X.: Cloud residues and interstitial aerosols from non-precipitating clouds over an industrial and urban area in northern China, Atmos. Environ., 45, 2488-2495, doi:10.1016/j.atmosenv.2011.02.044, 2011b.

Li, W. J., Zhou, S. Z., Wang, X. F., Xu, Z., Yuan, C., Yu, Y. C., Zhang, Q. Z., and Wang, W. X.: Integrated evaluation of aerosols from regional brown hazes over northern China in winter: Concentrations, sources, transformation, and mixing states, J. Geophys. Res., 116, 1-11, doi:10.1029/2010jd015099, 2011c.

Lin, Q., Zhang, G., Peng, L., Bi, X., Wang, X., Brechtel, F. J., Li, M., Chen, D., Peng, P., Sheng, G., and Zhou, Z.: In situ chemical composition measurement of individual cloud residue particles at a mountain site, southern China, Atmos. Chem. Phys., 17, 8473-8488, doi:10.5194/acp-17-8473-2017, 2017.

557 Matsui, H.: Black carbon simulations using a size- and mixing-state-resolved
558 three-dimensional model: 2. Aging timescale and its impact over East Asia, J. Geophys.
559 Res.-Atmos., 121, 1808-1821, doi:10.1002/2015jd023999, 2016.
560 McFiggans, G., Artaxo, P., Baltensperger, U., Coe, H., Facchini, M. C., Feingold, G.,
561 Fuzzi, S., Gysel, M., Laaksonen, A., Lohmann, U., Mentel, T. F., Murphy, D. M., O'Dowd, C.
562 D., Snider, J. R., and Weingartner, E.: The effect of physical and chemical aerosol properties on
563 warm cloud droplet activation, Atmos. Chem. Phys., 6, 2593-2649, 2006.
564 Moffet, R. C., and Prather, K. A.: In-situ measurements of the mixing state and optical
565 properties of soot with implications for radiative forcing estimates, Proc. Natl. Acad. Sci. USA,
566 106, 11872-11877, doi:10.1073/pnas.0900040106, 2009.
567 Peng, J. F., Hu, M., Guo, S., Du, Z. F., Zheng, J., Shang, D. J., Zamora, M. L., Zeng, L. M.,
568 Shao, M., Wu, Y. S., Zheng, J., Wang, Y., Glen, C. R., Collins, D. R., Molina, M. J., and Zhang,
569 R. Y.: Markedly enhanced absorption and direct radiative forcing of black carbon under
570 polluted urban environments, Proc. Natl. Acad. Sci. USA, 113, 4266-4271,
571 doi:10.1073/pnas.1602310113, 2016.
572 Petzold, A., Ogren, J. A., Fiebig, M., Laj, P., Li, S. M., Baltensperger, U., Holzer-Popp, T.,
573 Kinne, S., Pappalardo, G., Sugimoto, N., Wehrli, C., Wiedensohler, A., and Zhang, X. Y.:
574 Recommendations for reporting "black carbon" measurements, Atmos. Chem. Phys., 13,
575 8365-8379, 2013.
576 Qin, X. Y., Bhave, P. V., and Prather, K. A.: Comparison of two methods for obtaining
577 quantitative mass concentrations from aerosol time-of-flight mass spectrometry measurements,
578 Anal. Chem., 78, 6169-6178, doi:10.1021/ac060395q, 2006.
579 Qin, X. Y., Pratt, K. A., Shields, L. G., Toner, S. M., and Prather, K. A.: Seasonal
580 comparisons of single-particle chemical mixing state in Riverside, CA, Atmos. Environ., 59,
581 587-596, doi:10.1016/j.atmosenv.2012.05.032, 2012.
582 Roth, A., Schneider, J., Klimach, T., Mertes, S., van Pinxteren, D., Herrmann, H., and
583 Borrmann, S.: Aerosol properties, source identification, and cloud processing in orographic

584 clouds measured by single particle mass spectrometry on a central European mountain site
585 during HCCT-2010, Atmos. Chem. Phys., 16, 505-524, doi:10.5194/acp-16-505-2016, 2016.
586 Schroder, J. C., Hanna, S. J., Modini, R. L., Corrigan, A. L., Kreidenwies, S. M.,
587 Macdonald, A. M., Noone, K. J., Russell, L. M., Leaitch, W. R., and Bertram, A. K.:
588 Size-resolved observations of refractory black carbon particles in cloud droplets at a marine
589 boundary layer site, Atmos. Chem. Phys., 15, 1367-1383, doi:10.5194/acp-15-1367-2015,
590 2015.
591 Sellegri, K., Laj, P., Dupuy, R., Legrand, M., Preunkert, S., and Putaud, J. P.:
592 Size-dependent scavenging efficiencies of multicomponent atmospheric aerosols in clouds, J.
593 Geophys. Res.-Atmos., 108, 651-663, 2003.
594 Shingler, T., Dey, S., Sorooshian, A., Brechtel, F. J., Wang, Z., Metcalf, A., Coggon, M.,
595 Mulmenstadt, J., Russell, L. M., Jonsson, H. H., and Seinfeld, J. H.: Characterisation and
596 airborne deployment of a new counterflow virtual impactor inlet, Atmos. Meas. Tech., 5,
597 1259-1269, doi:10.5194/amt-5-1259-2012, 2012.
598 Song, X. H., Hopke, P. K., Fergenson, D. P., and Prather, K. A.: Classification of single
599 particles analyzed by ATOFMS using an artificial neural network, ART-2A, Anal. Chem., 71,
600 860-865, 1999.
601 Sorooshian, A., Wang, Z., Coggon, M. M., Jonsson, H. H., and Ervens, B.: Observations
602 of Sharp Oxalate Reductions in Stratocumulus Clouds at Variable Altitudes: Organic Acid and
603 Metal Measurements During the 2011 E-PEACE Campaign, Environ. Sci. Technol., 47,
604 7747-7756, doi:10.1021/es4012383, 2013.
605 Straub, D. J., Hutchings, J. W., and Herckes, P.: Measurements of fog composition at a
606 rural site, Atmos. Environ., 47, 195-205, doi:10.1016/j.atmosenv.2011.11.014, 2012.
607 van Pinxteren, D., Fomba, K. W., Mertes, S., Muller, K., Spindler, G., Schneider, J., Lee,
608 T., Collett, J. L., and Herrmann, H.: Cloud water composition during HCCT-2010: Scavenging
609 efficiencies, solute concentrations, and droplet size dependence of inorganic ions and dissolved
610 organic carbon, Atmos. Chem. Phys., 16, 3185-3205, doi:10.5194/acp-16-3185-2016, 2016.

Wang, Z., Wang, T., Guo, J., Gao, R., Xue, L. K., Zhang, J. M., Zhou, Y., Zhou, X. H., Zhang, Q. Z., and Wang, W. X.: Formation of secondary organic carbon and cloud impact on carbonaceous aerosols at Mount Tai, North China, Atmos. Environ., 46, 516-527, doi:10.1016/j.atmosenv.2011.08.019, 2012.

Weingartner, E., Saathoff, H., Schnaiter, M., Streit, N., Bitnar, B., and Baltensperger, U.: Absorption of light by soot particles: determination of the absorption coefficient by means of aethalometers, J. Aerosol Sci., 34, 1445-1463, doi:http://dx.doi.org/10.1016/S0021-8502(03)00359-8, 2003.

Wenzel, R. J., Liu, D. Y., Edgerton, E. S., and Prather, K. A.: Aerosol time-of-flight mass spectrometry during the Atlanta Supersite Experiment: 2. Scaling procedures, J. Geophys. Res.-Atmos., 108, 447-457, doi:10.1029/2001jd001563, 2003.

Wu, D., Wu, C., Liao, B., Chen, H., Wu, M., Li, F., Tan, H., Deng, T., Li, H., Jiang, D., and Yu, J. Z.: Black carbon over the South China Sea and in various continental locations in South China, Atmos. Chem. Phys., 13, 12257-12270, doi:10.5194/acp-13-12257-2013, 2013.

Xing, J. H., Takahashi, K., Yabushita, A., Kinugawa, T., Nakayama, T., Matsumi, Y., Tonokura, K., Takami, A., Imamura, T., Sato, K., Kawasaki, M., Hikida, T., and Shimono, A.: Characterization of Aerosol Particles in the Tokyo Metropolitan Area using Two Different Particle Mass Spectrometers, Aerosol Sci. Tech., 45, 315-326, doi:10.1080/02786826.2010.533720, 2011.

Yu, H., Wu, C., Wu, D., and Yu, J. Z.: Size distributions of elemental carbon and its contribution to light extinction in urban and rural locations in the pearl river delta region, China, Atmos. Chem. Phys., 10, 5107-5119, doi:10.5194/acp-10-5107-2010, 2010.

Zaveri, R. A., Barnard, J. C., Easter, R. C., Riemer, N., and West, M.: Particle-resolved simulation of aerosol size, composition, mixing state, and the associated optical and cloud condensation nuclei activation properties in an evolving urban plume, J. Geophys. Res.-Atmos., 115, 1383-1392, doi:10.1029/2009jd013616, 2010.

Zelenyuk, A., Imre, D., Earle, M., Easter, R., Korolev, A., Leaitch, R., Liu, P., Macdonald, A. M., Ovchinnikov, M., and Strapp, W.: In Situ Characterization of Cloud Condensation

639 Nuclei, Interstitial, and Background Particles Using the Single Particle Mass Spectrometer,
640 SPLAT II, Anal. Chem., 82, 7943-7951, doi:10.1021/Ac1013892, 2010.
641 Zhang, G., Lin, Q., Peng, L., Yang, Y., Fu, Y., Bi, X., Li, M., Chen, D., Chen, J., Cai, Z.,
642 Wang, X., Peng, P., Sheng, G., and Zhou, Z.: Insight into the in-cloud formation of oxalate
643 based on in situ measurement by single particle mass spectrometry, Atmos. Chem. Phys.
644 Discuss., 2017, 1-39, doi:10.5194/acp-2017-763, 2017.
645 Zhang, G. H., Bi, X. H., Chan, L. Y., Li, L., Wang, X. M., Feng, J. L., Sheng, G. Y., Fu, J.
646 M., Li, M., and Zhou, Z.: Enhanced trimethylamine-containing particles during fog events
647 detected by single particle aerosol mass spectrometry in urban Guangzhou, China, Atmos.
648 Environ., 55, 121-126, doi:10.1016/j.atmosenv.2012.03.038, 2012.
649 Zhang, G. H., Bi, X. H., Chan, L. Y., Wang, X. M., Sheng, G. Y., and Fu, J. M.:
650 Size-segregated chemical characteristics of aerosol during haze in an urban area of the Pearl
651 River Delta region, China, Urban Climate, 4, 74-84, doi:10.1016/j.uclim.2013.05.002, 2013.
652 Zhang, G. H., Bi, X. H., He, J. J., Chen, D. H., Chan, L. Y., Xie, G. W., Wang, X. M.,
653 Sheng, G. Y., Fu, J. M., and Zhou, Z.: Variation of secondary coatings associated with
654 elemental carbon by single particle analysis, Atmos. Environ., 92, 162-170,
655 doi:10.1016/j.atmosenv.2014.04.018, 2014.
656 Zhou, Y., Wang, T., Gao, X. M., Xue, L. K., Wang, X. F., Wang, Z., Gao, J. A., Zhang, Q.
657 Z., and Wang, W. X.: Continuous observations of water-soluble ions in PM2.5 at Mount Tai
658 (1534 ma.s.l.) in central-eastern China, J. Atmos. Chem., 64, 107-127, 2009.
659 Zuberi, B., Johnson, K. S., Aleks, G. K., Molina, L. T., and Laskin, A.: Hydrophilic
660 properties of aged soot, Geophys. Res. Lett., 32, 67-106, doi:10.1029/2004gl021496, 2005.
661

Atmos. Chem. Phys. Discuss., https://doi.org/10.5194/acp-2017-785
Manuscript under review for journal Atmos. Chem. Phys.
Discussion started: 25 August 2017

Atmospheric Chemistry and Physics Discussions

Figure captions

Fig. 1. Temporal profiles (with a 1 hour resolution) of $PM_{2.5}$, EBC mass concentrations, number of BC-containing particles by SPAMS, RH and visibility. Three cloud events are illustrated with black bars above the figure.

Fig. 2. Box and whisker plots of (a) concentration of EBC and (b) number fraction of BC-containing particles for each cloud event. In a box and whisker plot, the lower, median and upper lines of the box denote the 25^{th}, 50^{th}, and 75^{th} percentiles, respectively, and the lower and upper edges of the whisker denote the 10^{th} and 90^{th} percentiles, respectively.

Fig. 3. (a) Average mass spectrum of cloud RES BC-containing particles, and (b) the RPA ratios of ammonium, sulfate, nitrate, oxidized organic markers, and other organic markers (i.e., m/z 27$[C_2H_3]^+$, -26$[CN]^-$, 37$[C_3H]^+$, 50$[C_4H_2]^+$, 51$[C_4H_3]^+$, 61$[C_5H]^+$, and 63$[C_5H_3]^+$) to BC (carbon ion clusters ($C_n^{+/-}$, $n \leq 5$)), and the RPAs of BC for cloud RES and INT particles, respectively. Error bars represent the standard deviation in the hourly average RPA or the RPA ratios within a 95% confidence interval.

Fig. 4. Normalized number size distributions of the cloud-free, INT, and RES BC-containing particles. The data were averaged throughout the sampling period. The size distribution obtained from the SPMS is not representative of the actual aerosol size distribution due to the decreasing detection efficiencies at smaller sizes (Allen et al., 2000; Wenzel et al., 2003; Qin et al., 2006). A representative comparison between the size distributions measured by the SPAMS and the SPMS can be found in Fig. S12.

682 Fig. 5. Size-resolved Nf_{act} estimated for the BC-containing particles and all the detected
683 particles. The Nf_{act} is calculated as the ratio of the average number size distribution for the
684 cloud RES particles to the sum of the average number size distributions for the cloud RES and
685 INT particles. Errors were estimated assuming that the particle numbers detected by the
686 SPAMS follow a Poisson distribution.

687 Fig. 6. (a) Number fraction of each BC particle type in the cloud-free, INT, and RES
688 BC-containing particles, and (b) the number fraction of each BC particle type in the cloud
689 RES BC-containing particles separated for the three cloud events.

Atmos. Chem. Phys. Discuss., https://doi.org/10.5194/acp-2017-785
Manuscript under review for journal Atmos. Chem. Phys.
Discussion started: 25 August 2017

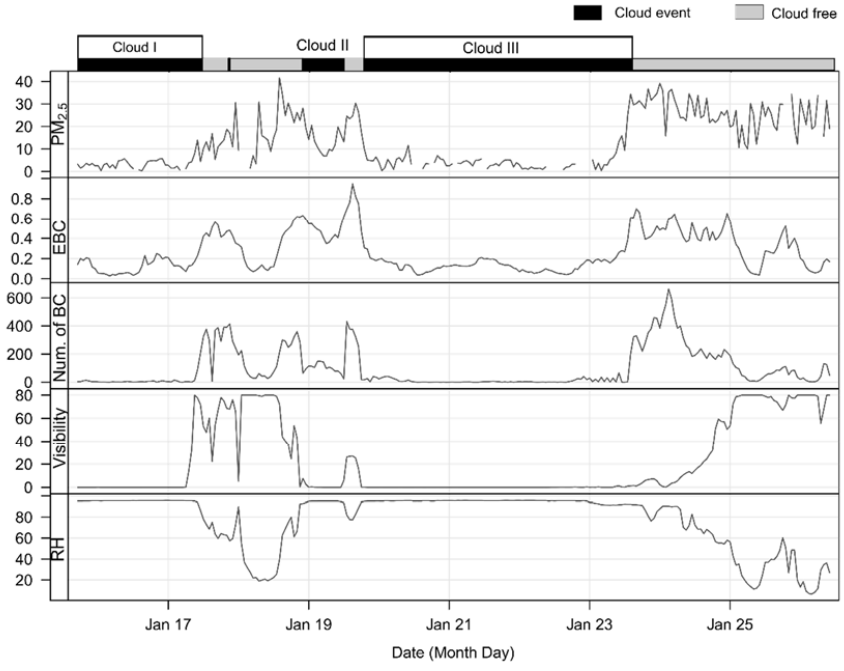

690

691 Fig. 1.

Atmos. Chem. Phys. Discuss., https://doi.org/10.5194/acp-2017-785
Manuscript under review for journal Atmos. Chem. Phys.
Discussion started: 25 August 2017

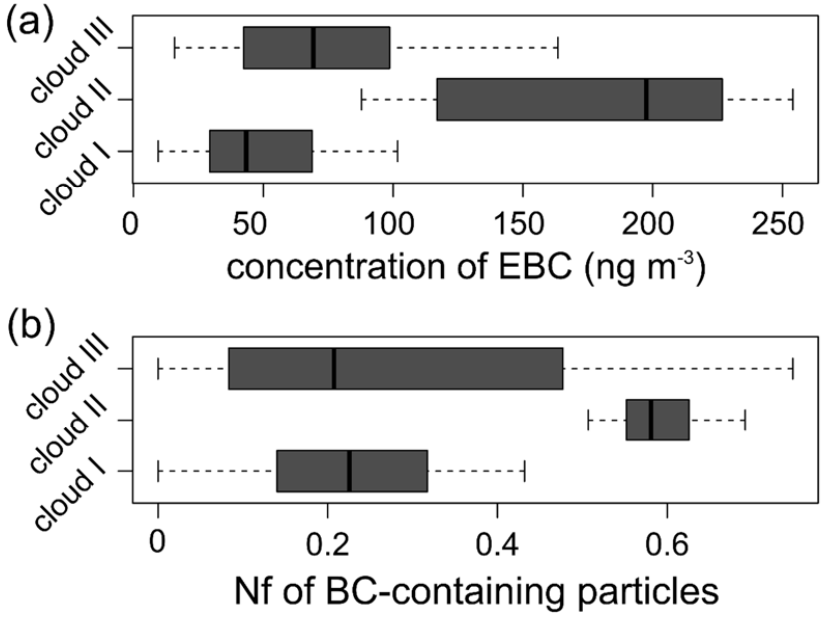

692

693 Fig. 2.

Atmos. Chem. Phys. Discuss., https://doi.org/10.5194/acp-2017-785
Manuscript under review for journal Atmos. Chem. Phys.
Discussion started: 25 August 2017

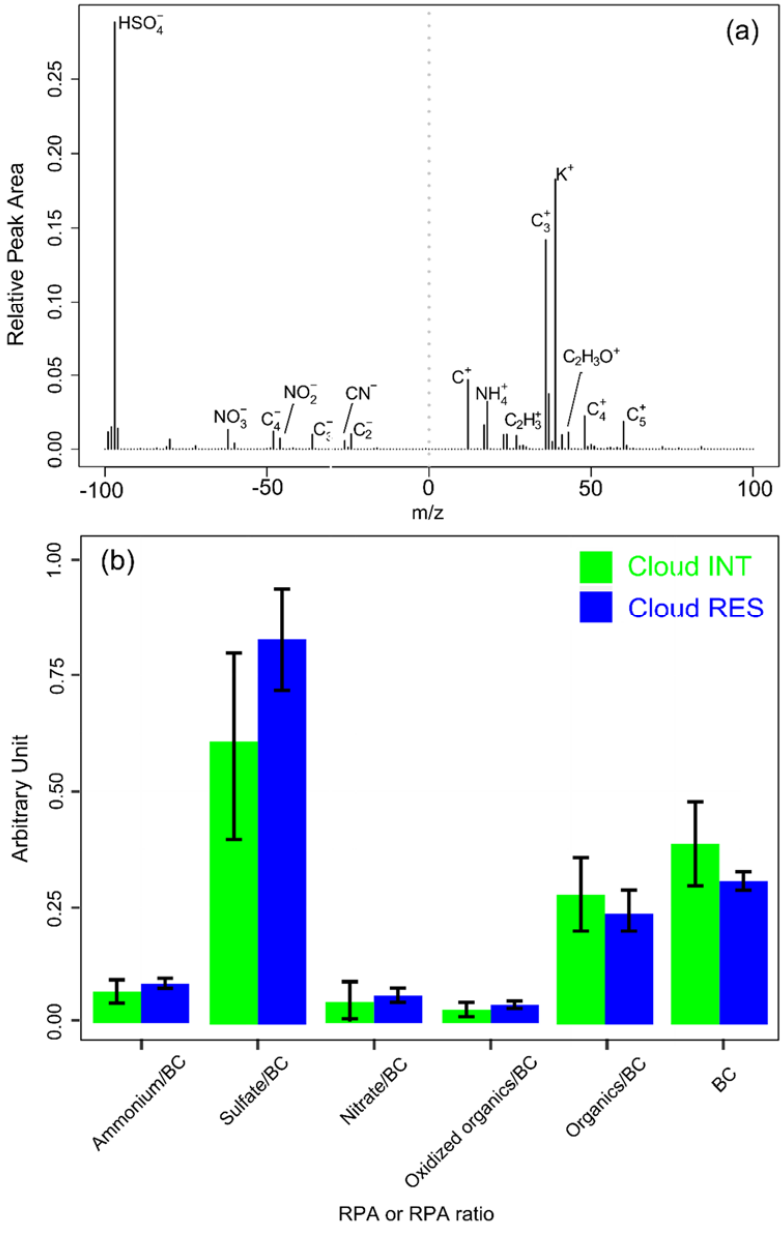

694

695 Fig. 3.

Atmos. Chem. Phys. Discuss., https://doi.org/10.5194/acp-2017-785
Manuscript under review for journal Atmos. Chem. Phys.
Discussion started: 25 August 2017

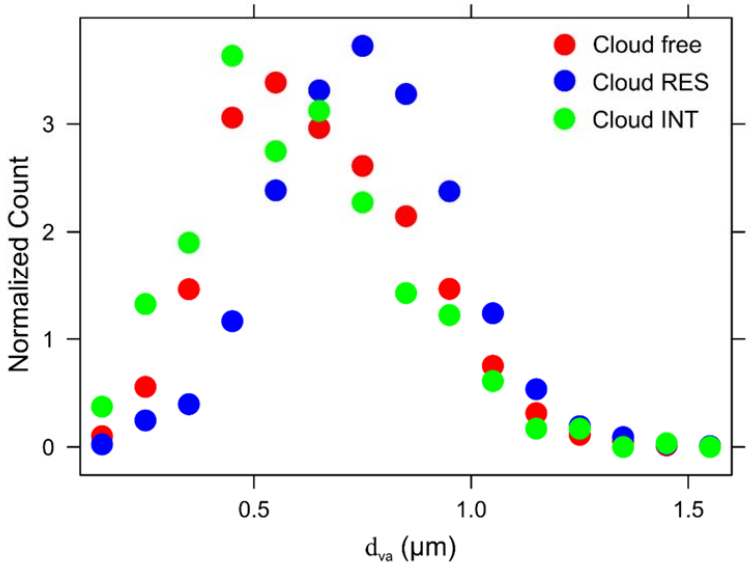

696

697 **Fig. 4.**

Atmos. Chem. Phys. Discuss., https://doi.org/10.5194/acp-2017-785
Manuscript under review for journal Atmos. Chem. Phys.
Discussion started: 25 August 2017

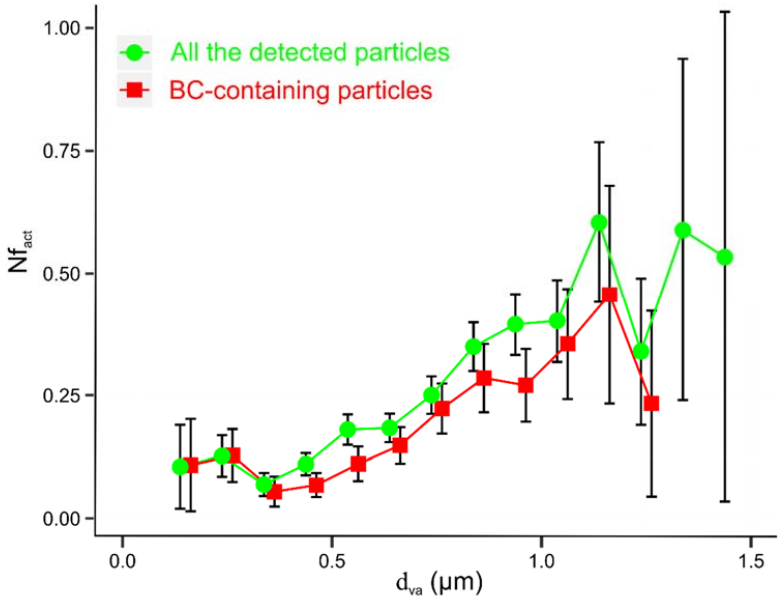

698

699 **Fig. 5.**

Atmos. Chem. Phys. Discuss., https://doi.org/10.5194/acp-2017-785
Manuscript under review for journal Atmos. Chem. Phys.
Discussion started: 25 August 2017

Atmospheric Chemistry and Physics Discussions

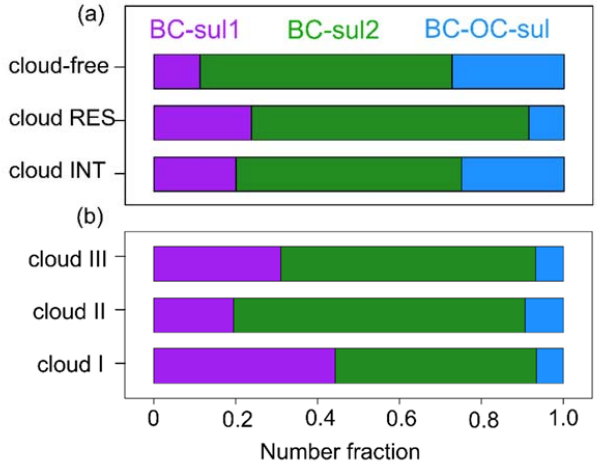

700

701 **Fig. 6.**

702